Journal of proteome research

Article

pubs.acs.org/jpr

Deciphering the Human Brain Proteome: Characterization of the Anterior Temporal Lobe and Corpus Callosum As Part of the Chromosome 15-centric Human Proteome Project

Daniel Martins-de-Souza,[*,†,‡,§,#] Paulo C. Carvalho,[∥,#] Andrea Schmitt,[†,§] Magno Junqueira,[⊥] Fábio C. S. Nogueira,[⊥] Christoph W. Turck,[‡] and Gilberto B. Domont[*,⊥]

[†]Research Group of Proteomics, Department of Psychiatry and Psychotherapy, Ludwig Maximilians University of Munich (LMU), Nußbaumstraße 7, Munich D-80336, Germany

[‡]Research Group of Proteomics and Biomarkers, Max Planck Institute of Psychiatry, Kraepelinstrasse 2, Munich 80804, Germany

[§]Laboratory of Neurosciences LIM-27, Department and Institute of Psychiatry, Faculty of Medicine, University of Sao Paulo, R. Dr. Ovídio Pires de Campos, 785 Caixa Postal 3671 - CEP 01060-970 São Paulo - SP - Brazil

[∥]Laboratory for Proteomics and Protein Engineering, Carlos Chagas Institute, Fiocruz, Rua Prof. Algacyr Munhoz Mader 3775, Curitiba 81350-010, Paraná, Brazil

[⊥]Proteomics Unit, Institute of Chemistry, Federal University of Rio de Janeiro (UFRJ), Avenida Athos da Silveira Ramos, Rio de Janeiro 21941-909, Brazil

Supporting Information

ABSTRACT: Defining the proteomes encoded by each chromosome and characterizing proteins related to human illnesses are among the goals of the Chromosome-centric Human Proteome Project (C-HPP) and the Biology and Disease-driven HPP. Following these objectives, we investigated the proteomes of the human anterior temporal lobe (ATL) and corpus callosum (CC) collected post-mortem from eight subjects. Using a label-free GeLC−MS/MS approach, we identified 2454 proteins in the ATL and 1887 in the CC through roughly 7500 and 5500 peptides, respectively. Considering that the ATL is a gray-matter region while the CC is a white-matter region, they presented proteomes specific to their functions. Besides, 38 proteins were found to be differentially expressed between the two regions. Furthermore, the proteome data sets were classified according to their chromosomal origin, and five proteins were evidenced at the MS level for the first time. We identified 70 proteins of the chromosome 15 − one of them for the first time by MS − which were submitted to an in silico pathway analysis. These revealed branch point proteins associated with Prader−Willi and Angelman syndromes and dyskeratosis congenita, which are chromosome-15-associated diseases. Data presented here can be a useful for brain disorder studies as well as for contributing to the C-HPP initiative. Our data are publicly available as resource data to C-HPP participant groups at http://yoda.iq.ufrj.br/Daniel/chpp2013. Additionally, the mass spectrometry proteomics data have been deposited to the ProteomeXchange with identifier PXD000547 for the corpus callosum and PXD000548 for the anterior temporal lobe.

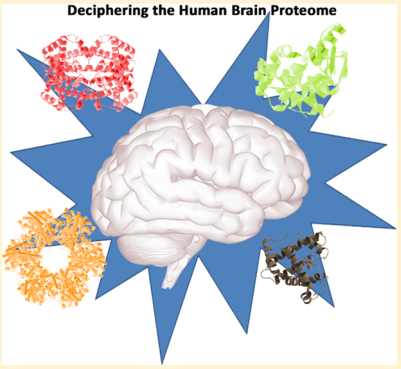

KEYWORDS: *chromosome 15, shotgun mass spectrometry, label-free, brain, neurosciences*

INTRODUCTION

In 2010, the Human Proteome Organization (HUPO) launched the Human Proteome Project (HPP) that similarly to the human genome project aims to map the entire human proteome.[1] One of the HPP's initiatives is the Chromosome-centric Human Proteome Project (C-HPP), whose main goal is to define the proteomes encoded by each chromosome.[2] Besides identification, the HPP and C-HPP also aim to characterize proteins related to human illnesses (Biology & Diseases, B/D Project),[3] which is of great interest considering their potential role for diagnosis, prognosis, treatment, and drug development.

Psychiatric disorders are one of the biggest burdens to the society. The World Health Organization (WHO, http://www.who.int) accounts that 3 of the 10 leading causes of disability in developed countries are due to psychiatric disorders such as depression, schizophrenia, and bipolar disorder. In comparison with other major health problems such as cancer and heart diseases, psychiatric disorders are neglected, most likely due to their nonfatal characteristics, despite their association with suicide. Additionally, monetary costs associated with healthcare and treatment noncompliance are significantly high[4,5] and are

Special Issue: Chromosome-centric Human Proteome Project

Received: September 8, 2013
Published: November 25, 2013

Table 1. Demographics of the Subjects Included in the Proteome Analyses[a]

sample ID	age (years)	gender	PMI (h)	pH values	cause of death	cigarettes per day	alcohol abuse
01	41	F	16	6.7	cardiopulmonary insufficiency	0	no
02	91	F	16	6.7	cardiopulmonary insufficiency	0	no
03	69	F	26	6.4	lung embolism	0	no
04	57	M	24	6.9	heart infarction	0	no
05	53	M	18	7.0	heart infarction	0	no
06	63	M	13	6.5	heart infarction	0	no
07	66	M	16	6.8	heart infarction	0	no
08	79	M	24	6.4	heart infarction	0	no

[a]Two pools for ATL and CC samples were composed of four samples each. Samples 1−4 comprised separate pools for ATL and CC, whereas 5−8 comprised other ATL and CC pools.

worsened by the fact that patients cannot work, decreasing their living standards.[6−8] Costs associated with psychiatric disorders can be as high as those incurred by heart disease and cancer.[9] Also, the WHO has projected that depression will become the main cause of disability for women and children by the year 2030 worldwide.[10]

Considering that psychiatric disorders are one of the most challenging fields of medical research, increased scientific efforts are still needed. The multifactorial characteristics of psychiatric disorders involve complex genetic, neurodevelopmental, environmental, and molecular components. The proteome is closely linked to the phenotype, and its analysis can deliver valuable information with regard to etiology.[11] In this line, HUPO also sponsors the Human Brain Proteome Project (HBPP), which aims for the characterization of the human brain proteome, focusing now on autopsies from human brains affected by neurodegenerative diseases. During the Human Proteome Meeting at the HUPO Congress 2013 in Yokohama, new data on the brain proteome project as well as a new genome-wide proteome project for the future biomedical sciences were presented.[12−14]

The current article is deals with the proteome characterization and comparison of two human brain regions − the anterior temporal lobe (ATL − Brodmann Area 38) and the corpus callosum (CC) − which were collected post-mortem from mentally healthy individuals. The ATL is a cortical region, mainly composed of neurons, which is involved in auditory and visual processing, language, and transfer from short- to long-term memory.[15] In contrast, the CC is mainly composed of white matter − glia and neuronal axons − that connects the cerebral hemispheres facilitating interhemispheric communication.[16] The present study not only contributes to the C-HPP efforts but also provides information for the study of psychiatric disorders. Additionally, this article goes along with the recently launched BRAIN Initiative by the NIH, whose main aim is to better understand the human brain.[17]

MATERIAL AND METHODS

Clinical Samples

Samples were collected post-mortem of the left ATL, Brodmann Area (BA) 38, and CC from eight subjects in the Institute of Neuropathology, Heidelberg University, Heidelberg, Germany. Brain samples were dissected by a neuropathologist and deep-frozen immediately after collection. Subjects had not suffered from psychiatric or neurological disorders, somatic diseases, or brain tumors and had never been treated with antidepressant or antipsychotic medications. Samples were submitted for neuropathologic characterization to rule out associated neurovascular or neurodegenerative disorders. Clinical records were collected from relatives and general practitioners. All subjects were German Caucasians and had no history of alcohol or drug abuse or severe physical illness. All assessments and post-mortem evaluations and procedures were approved by the ethics committee of the Faculty of Medicine of Heidelberg University, Heidelberg, Germany. Detailed patient information is given in Table 1.

Sample Preparation

About 20 mg of either ATL or CC tissue from the same subjects was homogenized in 100 μL of 7 M urea, 2 M thiourea, 4% CHAPS, 2% ASB-14, and 70 mM DTT using the Sample Grinding Kit (GE Healthcare, Munich, Germany). Samples were centrifuged for 10 min at 16 000*g* at 4 °C. The supernatants were collected, and protein concentrations were determined using the Bradford dye-binding assay (BioRad, Munich, Germany). We set up two pools for ATL and CC samples from eight subjects. Subjects 1−4 comprised separate ATL and CC pool, whereas 5−8 comprised other ATL and CC pools (Table 1).

Proteome Prefractionation

To enhance the proteome coverage, we employed SDS-PAGE for prefractionating the proteins prior to LC−MS analysis. Protein (40 μg) from a pooled sample was diluted in SDS-PAGE sample loading buffer (2% w/v SDS, 100 mM Tris (pH 6.8), 10% glycerol, 100 mM DTT, and 0.001% w/v bromophenol blue), heated for 5 min at 95 °C, and loaded in a 12% bis-tris polyacrylamide gel. Protein bands were visualized using Coomassie blue staining. Each gel lane containing stained protein bands was sliced equally into 20 sections. Each gel section was subjected to reduction and alkylation prior to in-gel digestion using trypsin. Resulting peptide mixtures were lyophilized prior to LC−MS.

LC−MS/MS

Extracted peptides were resuspended in 0.1% formic acid (FA) aqueous solution and separated using a nanoLC system (Eksigent, Dublin, CA) consisting of an autosampler and 2D-nano HPLC, coupled to an LTQ-Orbitrap XL mass spectrometer (Thermo Scientific, Bremen, Germany) equipped with a nano-ESI source. Samples were loaded onto a Zorbax-300 SB-C18 trapping column (5 μm, 5 × 0.3 mm i.d., Agilent Technologies, Santa Clara, CA) and washed for 10 min with 0.1% FA at 3 μL/min. Peptides were separated on a nanocolumn, 75 μm i.d. × 15 cm, PicoFrit capillary column (New Objective, Woburn, MA) packed in-house with 3 μm C18 coated particles (Dr. Maisch, Ammerbuch-Entringen, Germany). For liquid chromatography, 0.1% FA aqueous solvent (A) and ACN/0.1% FA (95/5 v/v) solvent (B) were used. The peptides were eluted with a linear gradient of solvent B from 2 to 10% in 5 min and from

dx.doi.org/10.1021/pr4009157 | J. Proteome Res. 2014, 13, 147−157

10 to 40% in 98 min at flow rate of 200 nL/min. The eluted peptides were analyzed online in ESI−MS and MS/MS positive modes. The mass spectrometer was set so that one full scan was acquired in the Orbitrap parallel to the MS/MS scans in the LTQ linear ion trap. The resolving power of the Orbitrap mass analyzer was set at resolution 60 000 (fmhw, m/z 400) for the precursor ion scan in the mass range 400 to 2000 Da. Fragmentation spectra (MS/MS mode) were acquired in data-dependent mode. The five most intense signal ions (m/z) per scan were selected for fragmentation with repeat duration time of 30 s, exclusion duration time of 60 s, isolation width (m/z) of 2 amu, activation time of 30 ms, activation Q 0.250, and normalized collision energy (V) 35. The chromatographic separation and spectra acquisition were performed in automatic mode, controlled and monitored by XCalibur software (version 2.0.7, Thermo Scientific, San Jose, CA).

Protein Identification and Quantification

Mass spectra were extracted in the MS2 format[18] using the PatternLab for Proteomics[19] RawReader (available at: http://proteomics.fiocruz.br/Softwares.aspx). The NeXtProt database was downloaded in August 2013. A target decoy database was then generated using PatternLab to include a reversed version of each sequence found in the database plus those from 127 common mass spectrometry contaminants. The ProLuCID search engine was used to compare experimental tandem mass spectra against those theoretically generated from our sequence database, followed by selection of the most likely peptide spectrum matches (PSMs). In brief, the search was limited to fully and semitryptic peptide candidates and imposed carbamidomethylation and oxidation of methionine as fixed and variable modifications, respectively. The search engine accepted peptide candidates within a 50 ppm tolerance from the measured precursor m/z and used the XCorr and Z-Score as the primary and secondary search engine scores, respectively. Identified proteins were classified according to their biological processes and molecular functions/classes using an in-house script that searches the Human Proteome Reference Database (http://www.hrpd.org: release 9, 30 047 protein entries, 41 327 protein−protein interactions, 112 158 protein expression, 22 490 subcellular localizations, 470 domains). To extract more information about unknown proteins, these were searched in GeneMania (http://www.genemania.org), a plugin of Cytoscape.[20]

Assessment of PSMs

The validity of the PSMs was assessed using the Search Engine Processor (SEPro).[21] Identifications were grouped by charge state (+2 and ≥+3) and then by tryptic status (fully tryptic, semitryptic), resulting in four distinct subgroups. For each result, the ProLuCID XCorr, DeltaCN, and Z-Score values were used to generate a Bayesian discriminator. The identifications were sorted in a nondecreasing order according to the discriminator score. A cutoff score was established to accept a false discovery rate (FDR) of 1% based on the number of labeled decoys. This procedure was independently performed on each data subset, resulting in an FDR that was independent of tryptic status or charge state. Additionally, a minimum sequence length of six amino acid residues was required. Results were postprocessed to only accept PSMs with <5 ppm and proteins supported by two or more independent evidences (e.g., identification of a peptide with different charge states, a modified and a nonmodified version of the same peptide, or two different peptides). Finally, we applied a new "one-hit-wonder" feature to SEPro (v. 2.1.0.21) that was incorporated in the tool and used for the first time in this report; proteins identified with only one PSM with an XCorr value <3 were eliminated.

Relative Protein Quantitation

The MS1 was extracted with RawReader and deconvoluted using YADA's default settings for bottom-up shotgun proteomics.[22] Extracted ion chromatograms (XICs) were obtained utilizing SEPro's Quantitation module, as previously described.[19] Subsequently, PatternLab's Regrouper module normalized the quantitative data according to the distributed normalized ion abundance factor (dNIAF)[23] approach, which is an adaptation of dNSAF[24] for XICs.

Pinpointing Differentially Expressed Proteins

We used PatternLab's approximately area proportional Venn diagram module to pinpoint proteins uniquely identified in a tissue; the analysis only considered proteins found in both technical replicates of each condition. As for proteins common to both biological replicates and also found in all replicates, we used PatternLab's TFold module using a q value of 0.01. The TFold module uses a theoretical FDR estimator to maximize identifications satisfying both a fold-change cutoff that varies with the t test p value as a power law and a stringency criterion that aims to fish out low abundant proteins that are likely to have had their quantitation compromised.[8]

RESULTS

Human Anterior Temporal Lobe Proteome

The two protein pools containing four samples each were submitted to the shotgun workflow, resulting in two ATL proteome data sets composed of 2805 and 2755 proteins, respectively, with FDRs lower than 1% identified from 7596 and 7338 unique peptides from 24 977 and 24 076 spectra, respectively. When combined, the ATL data sets had 2454 common proteins, which represents an 88% overlap between the two data sets, suggesting a highly reproducible shotgun-MS pipeline.

Human Corpus Callosum Proteome

The two pools of four CC samples each were analyzed by shotgun-MS. CC proteome data sets are composed of 2000 and 1967 proteins, respectively, with FDRs <1%, identified from 5334 and 5322 unique peptides from 21 023 and 20 788 spectra, respectively. The combination of CC proteome data sets resulted in 1887 common proteins, representing a 95% overlap between the two CC data sets.

Similarities and Differences between the Anterior Temporal Lobe and the Corpus Callosum Proteomes

The two brain regions here analyzed are essentially different: while the ATL is a cortical region, the CC is a white-matter region. Hence, each brain region presented a set of proteins that is unique to their proteome. Analyses of the ATL proteome showed 830 specific proteins, while 263 were observed in CC (Figure 1). Proteins were classified according to their biological processes (Figure 2). Both brain regions had proteins spanning nine distinct biological processes, which were differently represented according to their role in each region. We wish to emphasize that even though certain proteins were identified in only one brain region, this does not necessarily imply their absence in the other region. Their absence may be due to their low tissue abundance.

Even with such distinct characteristics, the ATL and CC tissues show a significant similarity of their proteomes. 1624 proteins

dx.doi.org/10.1021/pr4009157 | J. Proteome Res. 2014, 13, 147−157

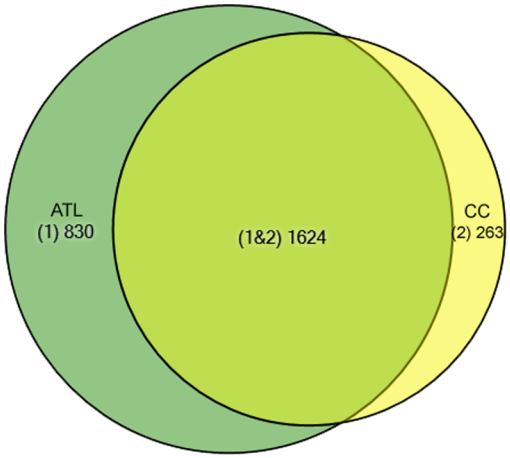

Figure 1. Venn diagram for the anterior temporal lobe (ATL) and corpus callosum (CC) proteomes. In the dark-green and yellow areas, proteins are specifically identified in the ATL and CC, respectively. In the middle are proteins that overlap between the two analyzed proteomes.

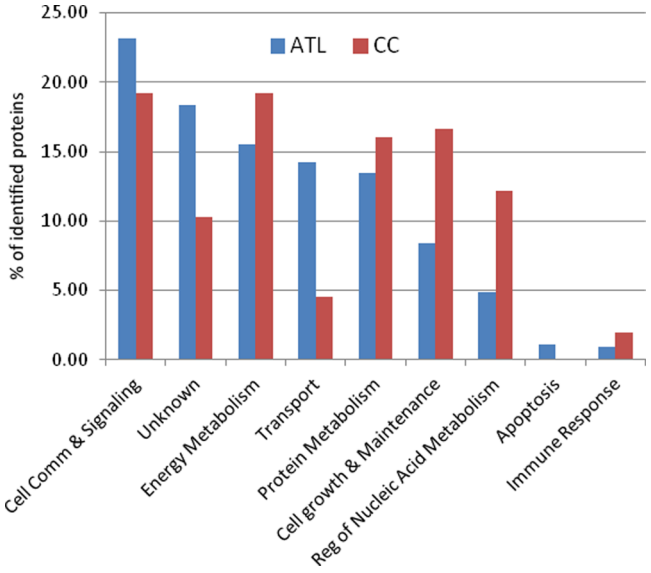

Figure 2. Biological processes of the unique proteins from anterior temporal lobe (ATL) and corpus callosum (CC) proteomes.

overlap between the ATL and CC, which represents ~66% of the ATL proteome and 86% of the CC proteome (Figure 1). Thirty-eight of the overlapping proteins presented a significant difference in abundance based on the TFold analysis (Table 2, Figure 3). These proteins are involved in seven different biological processes, with energy metabolism (42%) and cell communication and signaling (21%) the most prominent ones (Figure 4). These proteins belong to a number of molecular classes that are also involved in several different molecular functions (Table 2). The structural peculiarities of the ATL and CC are reflected in their proteomes. Large-fold differences (>30×) were observed for proteins associated with each brain region. While proteins such as cytochrome bc_1, protein kinase C, and casein kinase substrate in neurons 1, THY1 membrane glycoprotein, Syntaxin 1B2, and voltage-dependent anion-selective channel protein 1 are associated with the ATL, glial fibrillary acidic protein and Annexin I are associated with the CC.

Chromosomal Distribution of the CC and ATL

All four data sets were combined, and 2717 brain proteins were mapped, independently of the brain region. We classified these proteins according to their chromosomal origin (Figure 5), which can serve as a source for other participant groups of the HPP and more specifically to the C-HPP[1,2] (Supplementary Table 1 in the Supporting Information). Considering the particular focus of our group on chromosome 15, we have classified the 70 identified proteins that originated from this chromosome according to their biological processes and molecular functions (Table 3). 20% of these proteins are involved in cell growth and maintenance, and another 20% are involved in protein metabolism. It is noteworthy that 17% of the proteins are involved in energy metabolism and almost 13% have no defined functions. To obtain more information about these proteins, we have performed an in silico pathway analysis in GeneMania (Figure 6).

Unraveling Missing Proteins of the Human Proteome

ATL and CC mass spectrometric analysis provided evidence of five human proteins that are currently missing in NeXtProt. These are expressed by five different chromosomes (Table 4) and were identified by at least one unique peptide. Their mass spectra are available in the Supporting Information. Although our group focuses on chromosome 15, we make these data available to the other C-HPP groups.

DISCUSSION

Here we present the most complete proteome characterization of the human ATL and CC brain regions derived from a set of eight brains from mentally healthy subjects collected post-mortem. These data are publicly available and can be used as a resource of information including MS raw data, spectra, and protein identification results. The ATL data are of particularly interest for studying brain disorders such as Alzheimer's disease[25] and frontotemporal lobar degeneration.[26] The CC data have relevance for agenesis and schizophrenia.[27]

Considering that the ATL is mostly composed of neurons, while the CC is mostly composed of glia cells, we expected to identify sets of proteins that are specific for the individual brain regions. This was indeed the case, as can be seen in Figure 1. Proteins were classified according to their biological processes. Figure 2 reveals which biological processes were differentially represented in the two data sets of unique proteins. Transport proteins are more represented in the unique proteome of the ATL in comparison with the CC. This may be due to proteins that are mainly found in synapses, which mobilize a large machinery of intracellular and extracellular transport.[28] Cell growth and maintenance proteins are more present in the unique proteome of the CC. That is likely due to the structural role of glial cells such as myelinization and the pivotal role of the cytoskeleton in these cells.[29,30] We identified several protein components of the myelinization process such as myelin basic protein, myelin P2 protein, myelin proteolipid protein, and myelin-associated glycoprotein. These are classical markers for multiple sclerosis[31,32] that have also been found to be associated with schizophrenia.[33]

ATL and CC showed significant overlap in their proteomes (Figure 1), but, as expected, some of these proteins are present with differential abundance. The majority of differences observed in these brain regions are associated with energy metabolism processes (Table 2). As expected, 13 out of 16 proteins (81%) are more abundant in the ATL, because neurons have higher metabolic activity despite the neuronal metabolic dependency

dx.doi.org/10.1021/pr4009157 | J. Proteome Res. 2014, 13, 147−157

Table 2. Proteins Significantly Differentially Expressed between ATL and CC[a]

NextProt ID	UniProt ID	protein name	CC signal	ATL signal	FC (ATL/CC)	p value	biological process	molecular class	molecular function
nxp:NX_P14618−1	P14618	pyruvate kinase 3	4.27×10^{-3}	1.89×10^{-3}	−2.26	3.36×10^{-3}	energy metabolism	enzyme: phosphotransferase	kinase activity
nxp:NX_P00367−1	P00367	glutamate dehydrogenase 1	1.33×10^{-3}	4.24×10^{-3}	3.18	2.25×10^{-4}	energy metabolism	enzyme: dehydrogenase	catalytic activity
nxp:NX_P00441−1	P00441	superoxide dismutase [Cu−Zn]	1.43×10^{-3}	2.10×10^{-3}	1.47	1.67×10^{-3}	energy metabolism	enzyme: superoxide dismutase	superoxide dismutase activity
nxp:NX_P06576−1	P06576	ATP synthase, beta	7.00×10^{-4}	9.01×10^{-3}	12.87	2.13×10^{-5}	energy metabolism	transport/cargo protein	transporter activity
nxp:NX_P09104−1	P09104	enolase 2	1.16×10^{-3}	1.15×10^{-2}	9.93	1.19×10^{-3}	energy metabolism	enzyme: hydratase	catalytic activity
nxp:NX_P12277−1	P12277	creatine kinase brain type	9.06×10^{-3}	2.00×10^{-2}	2.20	1.52×10^{-3}	energy metabolism	enzyme: phosphotransferase	catalytic activity
nxp:NX_P15104−1	P15104	glutamate ammonia ligase	5.83×10^{-5}	2.16×10^{-3}	37.01	2.80×10^{-3}	energy metabolism	enzyme: aminotransferase	transaminase activity
nxp:NX_P21266−1	P21266	glutathione *S*-transferase Mu3	2.99×10^{-3}	1.46×10^{-3}	−2.04	2.23×10^{-3}	energy metabolism	enzyme: glutathione transferase	glutathione transferase activity
nxp:NX_P22695−1	P22695	ubiquinol cytochrome *c* reductase core protein II	8.09×10^{-5}	1.96×10^{-3}	24.25	3.92×10^{-4}	energy metabolism	enzyme: reductase	catalytic activity
nxp:NX_P25705−1	P25705	ATP synthase, H+ transporting, mitochondrial F1 complex, alpha subunit 1	1.31×10^{-3}	1.38×10^{-2}	10.54	1.08×10^{-4}	energy metabolism	transport/cargo protein	transporter activity
nxp:NX_P30041−1	P30041	peroxiredoxin 6	9.40×10^{-3}	2.82×10^{-3}	−3.34	1.22×10^{-3}	energy metabolism	enzyme: peroxidase	peroxidase activity
nxp:NX_P31930−1	P31930	cytochrome bc_1	2.14×10^{-5}	1.85×10^{-3}	>30	1.50×10^{-3}	energy metabolism	enzyme: reductase	catalytic activity
nxp:NX_P36957−1	P36957	dihydrolipoamide *s*-succinyl transferase	1.97×10^{-3}	7.82×10^{-3}	3.96	6.03×10^{-4}	energy metabolism	enzyme: acyltransferase	acyltransferase activity
nxp:NX_P38606−1	P38606	V-type proton ATPase catalytic subunit A	3.01×10^{-4}	3.27×10^{-3}	10.84	3.80×10^{-3}	energy metabolism	transport/cargo protein	transporter activity
nxp:NX_P40926−1	P40926	malate dehydrogenase mitochondrial	1.36×10^{-3}	1.25×10^{-2}	9.21	8.24×10^{-4}	energy metabolism	enzyme: dehydrogenase	catalytic activity
nxp:NX_P48735−1	P48735	isocitrate dehydrogenase 2	3.59×10^{-4}	2.14×10^{-3}	5.98	2.59×10^{-3}	energy metabolism	enzyme: dehydrogenase	catalytic activity
nxp:NX_P04083−1	P04083	annexin I	2.44×10^{-3}	5.22×10^{-5}	<30	3.88×10^{-3}	cell communication and signaling	calcium binding protein	calcium ion binding
nxp:NX_P21291−1	P21291	cysteine and glycine rich protein 1	2.94×10^{-3}	1.08×10^{-3}	−2.72	4.13×10^{-3}	cell communication and signaling	adapter molecule	receptor signaling complex scaffold
nxp:NX_P62158−1	P62158	calmodulin	2.46×10^{-4}	1.78×10^{-3}	7.24	4.29×10^{-3}	cell communication and signaling	calcium binding protein	calcium ion binding
nxp:NX_P62879−1	P62879	guanine nucleotide binding protein beta polypeptide 2	1.05×10^{-3}	1.89×10^{-3}	1.81	3.48×10^{-3}	cell communication and signaling	G protein	GTPase activity
nxp:NX_Q04917−1	Q04917	14-3-3 protein Eta	1.79×10^{-4}	3.32×10^{-3}	18.54	3.05×10^{-3}	cell communication and signaling	adapter molecule	receptor signaling complex scaffold
nxp:NX_Q13885−1	Q13885	tubulin beta-2A chain	5.76×10^{-3}	1.96×10^{-2}	3.41	6.99×10^{-4}	cell communication and signaling	cytoskeletal associated protein	cytoskeletal protein binding
nxp:NX_Q16555−1	Q16555	collapsin response mediator protein 2	1.13×10^{-2}	2.96×10^{-2}	2.63	1.05×10^{-3}	cell communication and signaling	cytoskeletal associated protein	cytoskeletal protein binding
nxp:NX_Q9BY11−1	Q9BY11	protein kinase C and casein kinase substrate in neurons 1	2.73×10^{-5}	1.69×10^{-3}	>30	4.31×10^{-3}	cell communication and signaling	adapter molecule	receptor signaling complex scaffold
nxp:NX_O94811−1	O94811	tubulin polymerization promoting protein	1.34×10^{-3}	4.32×10^{-3}	3.24	2.52×10^{-3}	cell growth and maintenance	cytoskeletal protein	structural constituent of cytoskeleton
nxp:NX_P04350−1	P04350	tubulin, beta 4	7.30×10^{-3}	2.03×10^{-2}	2.78	1.43×10^{-3}	cell growth and maintenance	cytoskeletal protein	structural constituent of cytoskeleton
nxp:NX_P08670−1	P08670	vimentin	1.32×10^{-2}	2.55×10^{-3}	−5.17	5.70×10^{-4}	cell growth and maintenance	cytoskeletal protein	structural constituent of cytoskeleton

dx.doi.org/10.1021/pr4009157 | J. Proteome Res. 2014, 13, 147−157

Table 2. continued

NextProt ID	UniProt ID	protein name	CC signal	ATL signal	FC (ATL/CC)	p value	biological process	molecular class	molecular function
nxp:NX_P14136–1	P14136	glial fibrillary acidic protein	5.95×10^{-01}	1.16×10^{-2}	<30	4.71×10^{-4}	cell growth and maintenance	structural protein	structural molecule activity
nxp:NX_P52565–1	P52565	rho GDP dissociation inhibitor alpha	8.43×10^{-4}	1.87×10^{-3}	2.21	1.81×10^{-3}	cell growth and maintenance	unclassified	molecular function unknown
nxp:NX_P04179–1	P04179	superoxide dismutase [Mn], mitochondrial	9.89×10^{-4}	1.78×10^{-3}	1.80	2.71×10^{-3}	cell growth and maintenance	enzyme: superoxide dismutase	superoxide dismutase activity
nxp:NX_P21281–1	P21281	V-type proton ATPase subunit B, brain isoform	2.14×10^{-4}	3.37×10^{-3}	15.79	4.62×10^{-5}	transport	transport/cargo protein	transporter activity
nxp:NX_P21796–1	P21796	voltage-dependent anion-selective channel protein 1	8.94×10^{-5}	6.82×10^{-3}	>30	5.83×10^{-5}	transport	voltage gated channel	voltage-gated ion channel activity
nxp:NX_P61266–1	P61266	syntaxin 1B2	1.66×10^{-5}	3.81×10^{-3}	>30	1.00×10^{-5}	transport	membrane transport protein	auxiliary transport protein activity
nxp:NX_Q9H115–1	Q9H115	beta soluble NSF attachment protein	1.19×10^{-4}	2.53×10^{-3}	21.34	5.13×10^{-4}	transport	unclassified	molecular function unknown
nxp:NX_O76070–1	O76070	synuclein, gamma	4.09×10^{-4}	1.96×10^{-3}	4.80	9.60×10^{-4}	protein metabolism	chaperone	chaperone activity
nxp:NX_P11142–1	P11142	heat shock 70 kDa protein 8	1.44×10^{-3}	5.70×10^{-3}	3.96	3.87×10^{-4}	protein metabolism	heat shock protein	heat shock protein activity
nxp:NX_P04216–1	P04216	Thy-1 membrane glycoprotein	2.27×10^{-5}	1.45×10^{-2}	>30	3.74×10^{-4}	immune response	unclassified	molecular function unknown
nxp:NX_Q9BW30–1	Q9BW30	CGI-38 brain specific protein	1.70×10^{-3}	1.54×10^{-4}	−11.01	3.81×10^{-3}	unknown	unclassified	molecular function unknown

[a]Sensitivity limit of our technique is able to distinguish fold changes up to 30.

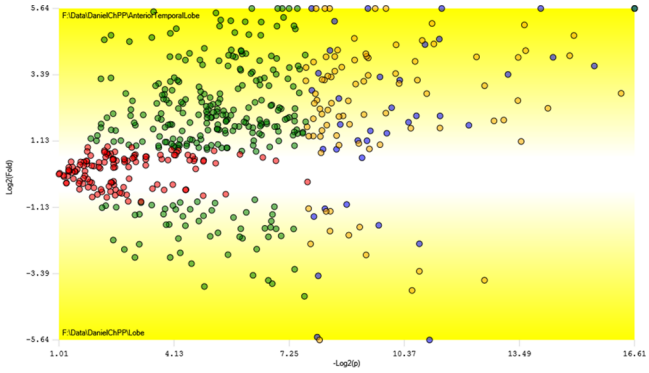

Figure 3. TFold comparison of ATL and CC. The TFold analysis considered proteins identified in all replicates. Each protein is mapped as a dot on the plot according to its p value) (x axis) and fold change (y axis). Proteins were quantitated according to the distributed normalized ion abundance factors. Red dots are proteins that satisfy neither the variable fold-change cutoff nor the FDR cutoff (q = 0.01). Green dots are those that satisfy the fold-change cutoff but not q. Orange dots are those that satisfy both the fold-change cutoff and q but are lowly abundant proteins and therefore could have their quantitation compromised. Finally, blue dots are those that satisfy all statistical filters. Dots in the upper part of the plot correspond to proteins up-regulated in the ATL.

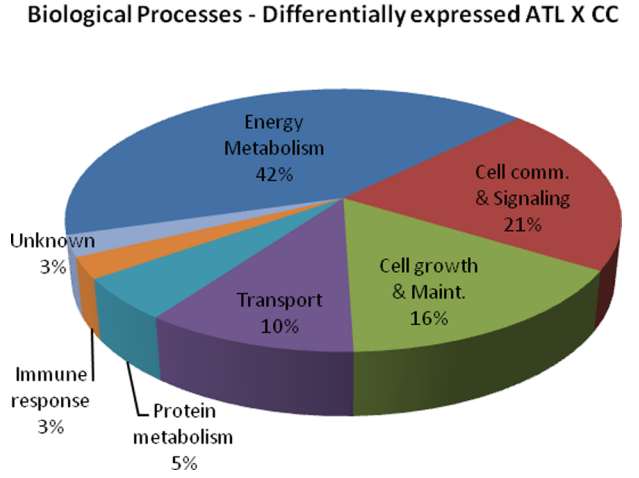

Figure 4. Differentially expressed proteins between the ATL and CC according to their biological processes, as described in Table 2.

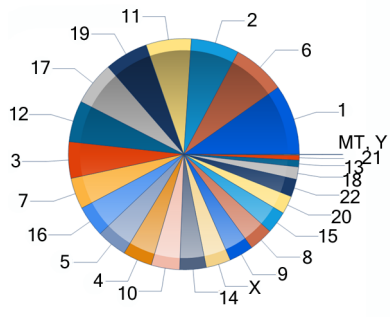

Figure 5. Proteome distribution according to chromosomal origin.

on glia.[34,35] Glia cells provide lactate to neurons as a source of energy,[34,35] which supports the high abundance of pyruvate kinase 3 in the CC. The downstream metabolic processes such as oxidative phosphorylation for ATP production, which is

dx.doi.org/10.1021/pr4009157 | J. Proteome Res. 2014, 13, 147−157

Table 3. Chromosome 15 Proteins Identified in Brain Proteome Data Sets[a]

UniProt ID	HPRD name	biological process	molecular class	molecular function
Q14696	mesoderm development candidate 2	cell growth and maintenance	chaperone	chaperone activity
Q9NZR1	tropomodulin 2	cell growth and maintenance	cytoskeletal associated protein	cytoskeletal protein binding
Q9Y3E1	hepatoma derived growth factor related protein 3	cell growth and maintenance	growth factor	growth factor activity
P78559	microtubule associated protein 1A	cell growth and maintenance	cytoskeletal associated protein	cytoskeletal protein binding
Q9UQ03	coronin 2B	cell growth and maintenance	cytoskeletal associated protein	cytoskeletal protein binding
P68032	actin alpha, cardiac muscle	cell growth and maintenance	cytoskeletal protein	structural constituent of cytoskeleton
P09493	tropomyosin 1 alpha chain	cell growth and maintenance	cytoskeletal associated protein	cytoskeletal protein binding
Q9Y4G6	talin 2	cell growth and maintenance	cytoskeletal associated protein	cytoskeletal protein binding
Q9Y4I1	myosin 5A	cell growth and maintenance	structural protein	structural molecule activity
Q8TDJ6	rabconnectin-3	cell growth and maintenance	structural protein	structural molecule activity
O15061	desmuslin	cell growth and maintenance	cytoskeletal protein	structural constituent of cytoskeleton
P46940	IQ motif containing GTPase activating protein 1	cell growth and maintenance	GTPase activating protein	GTPase activator activity
Q99963	SH3 containing GRB2 like protein 3	cell growth and maintenance	unclassified	molecular function unknown
Q96TC7	family with sequence similarity 82, member C	cell growth and maintenance	cell cycle control protein	apoptotic protease activator activity
Q96LD8	cysteine protease 2	protein metabolism	cysteine protease	cysteine-type peptidase activity
P32969	ribosomal protein L9	protein metabolism	ribosomal subunit	structural constituent of ribosome
P23284	peptidyl prolyl isomerase B	protein metabolism	chaperone	chaperone activity
P30101	protein disulfide isomerase A3	protein metabolism	enzyme: isomerase	isomerase activity
P25789	proteasome subunit, alpha type 4	protein metabolism	ubiquitin proteasome system protein	ubiquitin-specific protease activity
P37108	signal recognition particle 14 kDa	protein metabolism	RNA binding protein	RNA binding
P05386	ribosomal protein, large, P1	protein metabolism	ribosomal subunit	structural constituent of ribosome
O76031	ClpX caseinolytic protease X	protein metabolism	protease	peptidase activity
Q8WW22	DnaJ (Hsp40) homologue subfamily A member 4	protein metabolism	unclassified	molecular function unknown
P08708	ribosomal protein S17	protein metabolism	ribosomal subunit	structural constituent of ribosome
Q8WXD2	secretogranin III	protein metabolism	secreted polypeptide	molecular function unknown
O75822	eukaryotic translation initiation factor 3, subunit 1	protein metabolism	translation regulatory protein	translation regulator activity
P09668	cathepsin H	protein metabolism	cysteine protease	cysteine-type peptidase activity
P0CW22	40S ribosomal protein S17-like	protein metabolism	ribosomal subunit	structural constituent of ribosome
P14618	pyruvate kinase 3	energy metabolism	enzyme: phosphotransferase	kinase activity
Q00796	sorbitol dehydrogenase	energy metabolism	enzyme: dehydrogenase	catalytic activity
P50213	isocitrate dehydrogenase 3, alpha subunit	energy metabolism	enzyme: dehydrogenase	catalytic activity
P34949	mannose phosphate isomerase	energy metabolism	enzyme: isomerase	isomerase activity
P13804	electron transfer flavoprotein, alpha polypeptide	energy metabolism	membrane transport protein	auxiliary transport protein activity
P26440	isovaleryl coenzyme A dehydrogenase	energy metabolism	enzyme: dehydrogenase	catalytic activity
P48735	isocitrate dehydrogenase 2	energy metabolism	enzyme: dehydrogenase	catalytic activity
Q8N4P3	MGC45386	energy metabolism	enzyme: phosphohydrolase	catalytic activity
P16930	fumarylacetoacetase	energy metabolism	enzyme: hydrolase	hydrolase activity
P50440	AGAT	energy metabolism	enzyme: amidinotransferase	amidinotransferase activity
Q05086	ubiquitin protein ligase E3A	energy metabolism	ubiquitin proteasome system protein	ubiquitin-specific protease activity
P12532	creatine kinase U-type, mitochondrial	energy metabolism	enzyme: phosphotransferase	catalytic activity
Q99653	calcium binding protein P22	cell communication and signaling	calcium binding protein	calcium ion binding
P23677	inositol-trisphosphate 3-kinase A	cell communication and signaling	lipid kinase	lipid kinase activity
P59780	clathrin adaptor complex AP3, sigma 3B subunit	cell communication and signaling	adapter molecule	receptor signaling complex scaffold activity

dx.doi.org/10.1021/pr4009157 | J. Proteome Res. 2014, 13, 147−157

Table 3. continued

UniProt ID	HPRD name	biological process	molecular class	molecular function
Q02750	MEK1	cell communication and signaling	dual specificity kinase	protein threonine/tyrosine kinase activity
Q92930	RAB8B protein	cell communication and signaling	GTPase	GTPase activity
P43378	protein tyrosine phosphatase nonreceptor, type 9	cell communication and signaling	tyrosine phosphatase	protein tyrosine phosphatase activity
Q99828	calcium and integrin binding protein	cell communication and signaling	calcium binding protein	calcium ion binding
O14775	guanine nucleotide binding protein, beta 5	cell communication and signaling	G protein	GTPase activity
Q9NSB8	homer homologue 2	cell communication and signaling	unclassified	receptor signaling complex scaffold activity
P07355	annexin II	cell communication and signaling	calcium binding protein	calcium ion binding
P35398	RAR related orphan receptor A	reg. of nucleic acid metab	nuclear receptor	DNA binding
P33316	dUTP pyrophosphatase	reg. of nucleic acid metab	enzyme: hydrolase	hydrolase activity
P63162	small nuclear ribonucleoprotein polypeptide N	reg. of nucleic acid metab	ribonucleoprotein	ribonucleoprotein
P61201	thyroid hormone receptor interactor 15	reg. of nucleic acid metab	transcription regulatory protein	transcription regulator activity
P09661	U2A prime	reg. of nucleic acid metab	ribonucleoprotein	RNA binding
Q13367	adaptor related protein complex 3, beta-2 subunit	transport	transport/cargo protein	transporter activity
Q9UHW9	solute carrier family 12 member 6	transport	membrane transport protein	auxiliary transport protein activity
Q7L1I2	synaptic vesicle glycoprotein 2B	transport	membrane transport protein	auxiliary transport protein activity
Q8TAC9	secretory carrier membrane protein 5	transport	integral membrane protein	transporter activity
P39687	HLA DR associated protein I	immune response	MHC complex protein	MHC class I receptor activity
Q9Y639	stromal cell derived factor receptor 1	immune response	immunoglobulin	antigen binding
Q8N9N7	leucine rich repeat containing 57	unknown	unclassified	molecular function unknown
Q9GZS3	recombination protein REC14	unknown	unclassified	molecular function unknown
Q9NPA0	chromosome 15 open reading frame 24	unknown	unclassified	molecular function unknown
Q5GJ75	**tumor necrosis factor, alpha-induced protein 8-like 3**	**unknown**	**unclassified**	**molecular function unknown**
Q96FE5	leucine rich repeat neuronal 6A	unknown	unclassified	molecular function unknown
Q9H0A8	COMM domain containing protein 4	unknown	unclassified	molecular function unknown
Q5J8M3	transmembrane protein 85	unknown	unclassified	molecular function unknown
Q7Z6K5	chromosome 15 open reading frame 38	unknown	unclassified	molecular function unknown
Q7L576	cytoplasmic FMR1 interacting protein 1	unknown	unclassified	molecular function unknown

[a]C-HPP MasterTable (http://www.hprd.org/): release 9-27-2013, ver2, shows 70 out of 609 neXtProt entries of which 457 have neXtProt PE 1 protein level evidence (mass spectrometry only), 41 as PE 5 (dubious genes), leaving 111 as "missing". One missing protein with P1 evidence was found.

dx.doi.org/10.1021/pr4009157 | J. Proteome Res. 2014, 13, 147−157

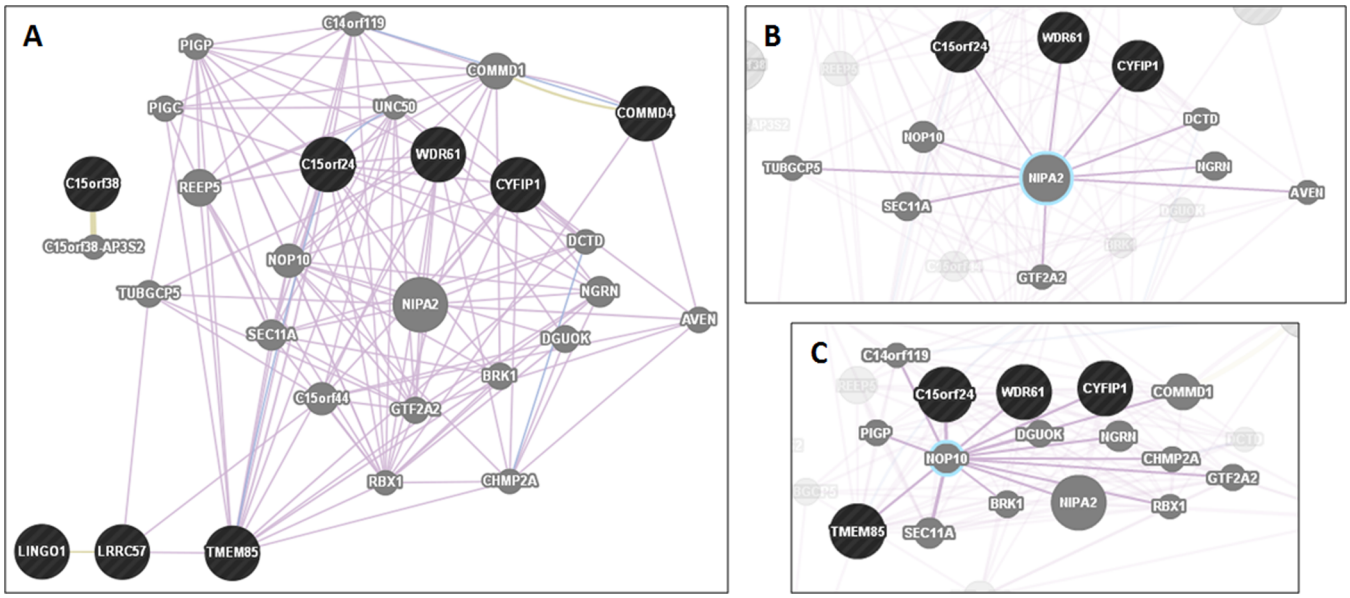

Figure 6. (A) Pathway analyses of the unknown protein from chromosome 15, highlighting the branch points (B) NIPA2 and (C) NOP10.

Table 4. Brain Proteins Identified for the First Time by Mass Spectrometry by at Least 1 Unique Peptide[a]

chromosome	NextProt ID	protein name	no. unique peptides
4	NX_Q8N9F0	*N*-acetylaspartate synthetase	1
6	NX_Q5JTD7	leucine-rich repeat-containing protein 73	2
11	NX_Q8IV01	synaptotagmin-12	2
14	NX_Q96NI6	leucine-rich repeat and fibronectin type-III domain-containing protein 5	1
15	**NX_Q5GJ75**	**tumor necrosis factor alpha-induced protein 8-like protein 3**	**1**

[a]Associated spectra are in the Supporting Information.

consumed during neuronal function, are completely performed in neurons, in agreement with the significant higher levels of cytochrome bc_1, ubiquinol cytochrome *c* reductase core protein II and ATP synthase, H+ transporting, mitochondrial F1 complex, and alpha subunit 1 in the ATL. Dysfunctions in energy processing through the differential expression of energy metabolism-related proteins have already been described in proteomic studies of brain disorders as schizophrenia[36] and depression[37] as well as ischemia,[38] Down syndrome,[39] fronto-temporal dementia,[40] and Alzheimer's disease.[41]

Regarding the different abundance of proteins involved in cell communication and signaling, the high abundance of annexin A1 in CC confirms this protein as a marker for astrocytes[42] and microglia.[43] Other proteins that are more abundant in ATL include protein kinase C and casein kinase substrate in neuron 1. Its abundance is >30 fold higher and signals to the organization of the cytoskeleton via MAPT and participates in cellular transport by recruiting DNM1, DNM2, and DNM3, which are pivotal for synaptic transmission.[44] Also involved in synaptic processes are voltage-dependent anion-selective channel protein 1 and Syntaxin 1B2, which are also very abundant in the ATL due to its characteristic gray-matter brain region. Other classical glial markers such as glial fibrillary acidic protein show higher abundance in CC. The most significant difference observed was for Thy-1 membrane glycoprotein, which is >30× more abundant in the ATL than in CC. This protein participates in synaptogenesis, which explains its larger abundance.[45] Additionally, THY1 has been recently associated with fear inhibition in the amygdala.[46]

ATL and CC proteomes were classified according to their chromosomal origin (Figure 5). We have identified 70 proteins originating from chromosome 15, which is the central interest of our work group. Regarding the biological processes, more than half of them belong to cellular processes such as cell growth and maintenance, protein metabolism, and energy metabolism (Table 3). However, the most intriguing part of this data is the identification of proteins from chromosome 15 with unknown biological or molecular function. An in silico analysis of these proteins by GeneMania proposes an intricate network of interactions (Figure 6A). However, 90.4% of this network (purple lines) is based on previous reports that coidentified these genes or proteins. This is not very informative, but two particular branch points of this network may exist. One is the branch point NIPA2 (nonimprinted in Prader–Willi/Angelman syndrome region protein 2) (Figure 6B). Interestingly, NIPA2 is a product of chromosome 15, only verified at the transcriptional level, and may be associated with Prader–Willi and Angelman syndromes,[47] which are rare genetic disorders associated with chromosome 15. Another branch point is NOP10 (H/ACA ribonucleoprotein complex subunit 3) (Figure 6C). This protein is involved in ribosome production and maintenance of telomeres.[48] A mutation in a highly conserved region of the Nop10 sequence, which is also part of chromosome 15, may lead to dyskeratosis congenita, a condition caused by dysfunction in the maintenance of the telomeres.[49]

Among the unknown proteins, we find tumor necrosis factor alpha-induced protein 8-like protein 3 (TNFAIP8L3), a product of chromosome 15 that has evidence of existence only at the transcript level (http://www.uniprot.org/uniprot/Q5GJ75). This cytosolic protein[50] belongs to the TNFAIP8 family, which regulates apoptosis negatively and participates in tumor

dx.doi.org/10.1021/pr4009157 | J. Proteome Res. 2014, 13, 147–157

progression processes.[51,52] We also identified four other proteins for the first time by MS with other chromosomal origin (Table 4).

In summary, we present the proteome characterization of ATL and CC, which may be informative for studies aimed at the elucidation of neurological processes, and complement the existing knowledge of brain biochemistry and function. As a contribution to the C-HPP initiative, we could detect for the first time by MS five proteins from chromosomes 4, 6, 11, 14, and 15, which are available as a resource for other groups' interests.

■ ASSOCIATED CONTENT

Supporting Information

Genes and annotated proteins from human chromosomes extracted from NeXtProt for 2.717 different proteins identified in this work.

Mass spectra of five human proteins identified by at least one unique peptide currently missing in NeXtProt and expressed by five different chromosomes. This material is available free of charge via the Internet at http://pubs.acs.org. The RAW data together with all identification (SEPro files *.sepr) are available for download at http://yoda.iq.ufrj.br/Daniel/chpp2013. The SEPro provides a graphical user interface to dynamically view the identified proteins together with their corresponding peptides and annotated mass spectra. Additionally, the mass spectrometry proteomics data have been deposited to the ProteomeXchange Consortium (http://proteomecentral.proteomexchange.org) via the PRIDE partner repository[53] with the data set identifier PXD000547 for the corpus callosum and PXD000548 for the anterior temporal lobe.

■ AUTHOR INFORMATION

Corresponding Authors

*D.M.-d.-S.: Tel: +49 89 30622-630. Fax: +49 89 30622-200.
*G.B.D.: Tel: +55 21 2562-7353. Fax: +55 21 2562-7353.

Author Contributions

#D.M.-d.-S. and P.C.C. contributed equally.

Notes

The authors declare no competing financial interest.

■ ACKNOWLEDGMENTS

P.C.C. was funded by Conselho Nacional de Desenvolvimento Científico e Tecnológico (CNPq) and RPT02H PDTIS/Carlos Chagas Institute − Fiocruz, Parana. G.B.D. acknowledges support from FAPERJ (E-26/110.138/2013) and CNPq (BP 308819/2011).

■ REFERENCES

(1) Legrain, P.; Aebersold, R.; Archakov, A.; Bairoch, A.; Bala, K.; Beretta, L.; Bergeron, J.; Borchers, C. H.; Corthals, G. L.; Costello, C. E.; Deutsch, E. W.; Domon, B.; Hancock, W.; He, F.; Hochstrasser, D.; Marko-Varga, G.; Salekdeh, G. H.; Sechi, S.; Snyder, M.; Srivastava, S.; Uhlen, M.; Wu, C. H.; Yamamoto, T.; Paik, Y. K.; Omenn, G. S. The human proteome project: current state and future direction. *Mol. Cell. Proteomics* **2011**, *10* (7), M111 009993.

(2) Paik, Y. K.; Jeong, S. K.; Omenn, G. S.; Uhlen, M.; Hanash, S.; Cho, S. Y.; Lee, H. J.; Na, K.; Choi, E. Y.; Yan, F.; Zhang, F.; Zhang, Y.; Snyder, M.; Cheng, Y.; Chen, R.; Marko-Varga, G.; Deutsch, E. W.; Kim, H.; Kwon, J. Y.; Aebersold, R.; Bairoch, A.; Taylor, A. D.; Kim, K. Y.; Lee, E. Y.; Hochstrasser, D.; Legrain, P.; Hancock, W. S. The Chromosome-Centric Human Proteome Project for cataloging proteins encoded in the genome. *Nat. Biotechnol.* **2012**, *30* (3), 221−3.

(3) Aebersold, R.; Bader, G. D.; Edwards, A. M.; van Eyk, J. E.; Kussmann, M.; Qin, J.; Omenn, G. S. The biology/disease-driven human proteome project (B/D-HPP): enabling protein research for the life sciences community. *J. Proteome Res.* **2013**, *12* (1), 23−7.

(4) Bahn, S.; Schwarz, E.; Harris, L. W.; Martins-de-Souza, D.; Rahmoune, H.; Guest, P. C. Biomarker blood tests for diagnosis and management of mental disorders: focus on schizophrenia. *Rev. Psiq. Clín.* **2013**, *40* (1), 7.

(5) Greenberg, P. E.; Kessler, R. C.; Birnbaum, H. G.; Leong, S. A.; Lowe, S. W.; Berglund, P. A.; Corey-Lisle, P. K. The economic burden of depression in the United States: how did it change between 1990 and 2000? *J. Clin. Psychiatry* **2003**, *64* (12), 1465−75.

(6) Gibb, S. J.; Fergusson, D. M.; Horwood, L. J. Burden of psychiatric disorder in young adulthood and life outcomes at age 30. *Br. J. Psychiatry* **2010**, *197* (2), 122−7.

(7) Arends, I.; Bultmann, U.; van Rhenen, W.; Groen, H.; van der Klink, J. J. Economic evaluation of a problem solving intervention to prevent recurrent sickness absence in workers with common mental disorders. *PLoS One* **2013**, *8* (8), e71937.

(8) Insel, T. R. Assessing the economic costs of serious mental illness. *Am. J. Psychiatry* **2008**, *165* (6), 663−5.

(9) Suliman, S.; Stein, D. J.; Myer, L.; Williams, D. R.; Seedat, S. Disability and treatment of psychiatric and physical disorders in South Africa. *J. Nerv. Ment. Dis.* **2010**, *198* (1), 8−15.

(10) Hindi, F.; Dew, M. A.; Albert, S. M.; Lotrich, F. E.; Reynolds, C. F., 3rd Preventing depression in later life: state of the art and science circa 2011. *Psychiatr. Clin. North Am.* **2011**, *34* (1), 67−78.

(11) Martins-de-Souza, D. Proteomics tackling schizophrenia as a pathway disorder. *Schizophr. Bull.* **2012**, *38* (6), 1107−8.

(12) Meyer, H. E., May, C., Schrötter, A., Turewitz, M., Eisenacher, M., Woitalla, D., Heinsen, H., Wiltfang, J., Leite, R., Grinberg, L. T. In *Biomarker Discovery for Alzheimer and Parkinson Disease*, HUPO 12th Annual World Congress, Yokohama, Japan, 2013.

(13) Magraoui, F. E., Heinsen, H., Mastalski, T., Seger, S., Eisenacher, M., Leite, R. E., Grinberg, L. T., Kuhlmann, K., Meyer, H. E., Schroetter, A. In *Differential Proteomic Analysis of Human Hippocampal Regions of Interest (CA1, CA2, CA3, fascia dentata) - Relevance for Alzheimer's Disease*, HUPO 12th Annual World Congress, Yokohama, Japan, 2013.

(14) Jeong, S.-K., Lee, H.-J., Na, K., Hancock, W. S., Paik, Y.-K. In *A New Genome-Wide Proteome Project for the Future Biomedical Sciences Proteomic Expression Data for the Placenta within the Genomewide PDB*, HUPO 12th Annual World Congress, Yokohama, Japan, 2013; Yokohama, Japan, 2013.

(15) Wong, C.; Gallate, J. The function of the anterior temporal lobe: a review of the empirical evidence. *Brain Res.* **2012**, *1449*, 94−116.

(16) Wahl, M.; Lauterbach-Soon, B.; Hattingen, E.; Jung, P.; Singer, O.; Volz, S.; Klein, J. C.; Steinmetz, H.; Ziemann, U. Human motor corpus callosum: topography, somatotopy, and link between microstructure and function. *J. Neurosci.* **2007**, *27* (45), 12132−8.

(17) Insel, T. R.; Landis, S. C.; Collins, F. S. Research priorities. The NIH BRAIN Initiative. *Science* **2013**, *340* (6133), 687−8.

(18) McDonald, W. H.; Tabb, D. L.; Sadygov, R. G.; MacCoss, M. J.; Venable, J.; Graumann, J.; Johnson, J. R.; Cociorva, D.; Yates, J. R., 3rd. MS1, MS2, and SQT-three unified, compact, and easily parsed file formats for the storage of shotgun proteomic spectra and identifications. *Rapid Commun. Mass Spectrom.* **2004**, *18* (18), 2162−8.

(19) Carvalho, P. C.; Fischer, J. S.; Xu, T.; Yates, J. R., 3rd; Barbosa, V. C. PatternLab: from mass spectra to label-free differential shotgun proteomics. In *Current Protocols in Bioinformatics*; Wiley: New York, 2012, Chapter 13, Unit 13.19.

(20) Saito, R.; Smoot, M. E.; Ono, K.; Ruscheinski, J.; Wang, P. L.; Lotia, S.; Pico, A. R.; Bader, G. D.; Ideker, T. A travel guide to Cytoscape plugins. *Nat. Methods* **2012**, *9* (11), 1069−76.

(21) Carvalho, P. C.; Fischer, J. S.; Xu, T.; Cociorva, D.; Balbuena, T. S.; Valente, R. H.; Perales, J.; Yates, J. R., 3rd; Barbosa, V. C. Search

engine processor: filtering and organizing peptide spectrum matches. *Proteomics* **2012**, *12* (7), 944−9.
(22) Carvalho, P. C.; Xu, T.; Han, X.; Cociorva, D.; Barbosa, V. C.; Yates, J. R., 3rd. YADA: a tool for taking the most out of high-resolution spectra. *Bioinformatics* **2009**, *25* (20), 2734−6.
(23) Aquino, P. F.; Fischer, J. S.; Neves-Ferreira, A. G.; Perales, J.; Domont, G. B.; Araujo, G. D.; Barbosa, V. C.; Viana, J.; Chalub, S. R.; Lima de Souza, A. Q.; Carvalho, M. G.; Leao de Souza, A. D.; Carvalho, P. C. Are gastric cancer resection margin proteomic profiles more similar to those from controls or tumors? *J. Proteome Res.* **2012**, *11* (12), 5836−42.
(24) Zhang, Y.; Wen, Z.; Washburn, M. P.; Florens, L. Refinements to label free proteome quantitation: how to deal with peptides shared by multiple proteins. *Anal. Chem.* **2010**, *82* (6), 2272−81.
(25) Domoto-Reilly, K.; Sapolsky, D.; Brickhouse, M.; Dickerson, B. C. Naming impairment in Alzheimer's disease is associated with left anterior temporal lobe atrophy. *Neuroimage* **2012**, *63* (1), 348−55.
(26) Sieben, A.; Van Langenhove, T.; Engelborghs, S.; Martin, J. J.; Boon, P.; Cras, P.; De Deyn, P. P.; Santens, P.; Van Broeckhoven, C.; Cruts, M. The genetics and neuropathology of frontotemporal lobar degeneration. *Acta Neuropathol.* **2012**, *124* (3), 353−72.
(27) Paul, L. K.; Brown, W. S.; Adolphs, R.; Tyszka, J. M.; Richards, L. J.; Mukherjee, P.; Sherr, E. H. Agenesis of the corpus callosum: genetic, developmental and functional aspects of connectivity. *Nat. Rev. Neurosci.* **2007**, *8* (4), 287−99.
(28) O'Rourke, N. A.; Weiler, N. C.; Micheva, K. D.; Smith, S. J. Deep molecular diversity of mammalian synapses: why it matters and how to measure it. *Nat. Rev. Neurosci.* **2012**, *13* (6), 365−79.
(29) Potokar, M.; Kreft, M.; Li, L.; Daniel Andersson, J.; Pangrsic, T.; Chowdhury, H. H.; Pekny, M.; Zorec, R. Cytoskeleton and vesicle mobility in astrocytes. *Traffic* **2007**, *8* (1), 12−20.
(30) Richter-Landsberg, C. The cytoskeleton in oligodendrocytes. Microtubule dynamics in health and disease. *J. Mol. Neurosci.* **2008**, *35* (1), 55−63.
(31) Lassmann, H.; van Horssen, J. The molecular basis of neurodegeneration in multiple sclerosis. *FEBS Lett.* **2011**, *585* (23), 3715−23.
(32) Farias, A. S.; Pradella, F.; Schmitt, A.; Barbosa, L. M.; Martins-de-Souza, D., Ten Years of Proteomics in Multiple Sclerosis. *Proteomics* **2014**, *14*, (2).
(33) Martins-de-Souza, D. Proteome and transcriptome analysis suggests oligodendrocyte dysfunction in schizophrenia. *J. Psychiatr. Res.* **2010**, *44* (3), 149−56.
(34) Bouzier-Sore, A. K.; Merle, M.; Magistretti, P. J.; Pellerin, L. Feeding active neurons: (re)emergence of a nursing role for astrocytes. *J. Physiol. (Paris)* **2002**, *96* (3−4), 273−82.
(35) Funfschilling, U.; Supplie, L. M.; Mahad, D.; Boretius, S.; Saab, A. S.; Edgar, J.; Brinkmann, B. G.; Kassmann, C. M.; Tzvetanova, I. D.; Mobius, W.; Diaz, F.; Meijer, D.; Suter, U.; Hamprecht, B.; Sereda, M. W.; Moraes, C. T.; Frahm, J.; Goebbels, S.; Nave, K. A. Glycolytic oligodendrocytes maintain myelin and long-term axonal integrity. *Nature* **2012**, *485* (7399), 517−21.
(36) Martins-de-Souza, D.; Harris, L. W.; Guest, P. C.; Bahn, S. The role of energy metabolism dysfunction and oxidative stress in schizophrenia revealed by proteomics. *Antioxid. Redox Signaling* **2011**, *15* (7), 2067−79.
(37) Martins-de-Souza, D.; Guest, P. C.; Harris, L. W.; Vanattou-Saifoudine, N.; Webster, M. J.; Rahmoune, H.; Bahn, S. Identification of proteomic signatures associated with depression and psychotic depression in post-mortem brains from major depression patients. *Transl. Psychiatry* **2012**, *2*, e87.
(38) Villa, R. F.; Gorini, A.; Ferrari, F.; Hoyer, S. Energy metabolism of cerebral mitochondria during aging, ischemia and post-ischemic recovery assessed by functional proteomics of enzymes. *Neurochem. Int.* **2013**, *63*, 765−781.
(39) Di Domenico, F.; Coccia, R.; Cocciolo, A.; Murphy, M. P.; Cenini, G.; Head, E.; Butterfield, D. A.; Giorgi, A.; Schinina, M. E.; Mancuso, C.; Cini, C.; Perluigi, M. Impairment of proteostasis network in Down syndrome prior to the development of Alzheimer's disease neuropathology: redox proteomics analysis of human brain. *Biochim. Biophys. Acta* **2013**, *1832* (8), 1249−59.
(40) Martins-de-Souza, D.; Guest, P. C.; Mann, D. M.; Roeber, S.; Rahmoune, H.; Bauder, C.; Kretzschmar, H.; Volk, B.; Baborie, A.; Bahn, S. Proteomic analysis identifies dysfunction in cellular transport, energy, and protein metabolism in different brain regions of atypical frontotemporal lobar degeneration. *J. Proteome Res.* **2012**, *11* (4), 2533−43.
(41) Sultana, R.; Butterfield, D. A. Oxidative modification of brain proteins in Alzheimer's disease: perspective on future studies based on results of redox proteomics studies. *J. Alzheimers Dis.* **2013**, *33* (Suppl 1), S243−51.
(42) Schittenhelm, J.; Trautmann, K.; Tabatabai, G.; Hermann, C.; Meyermann, R.; Beschorner, R. Comparative analysis of annexin-1 in neuroepithelial tumors shows altered expression with the grade of malignancy but is not associated with survival. *Mod. Pathol.* **2009**, *22* (12), 1600−11.
(43) McArthur, S.; Cristante, E.; Paterno, M.; Christian, H.; Roncaroli, F.; Gillies, G. E.; Solito, E. Annexin A1: a central player in the anti-inflammatory and neuroprotective role of microglia. *J. Immunol.* **2010**, *185* (10), 6317−28.
(44) Yamashita, T. Ca2+-dependent regulation of synaptic vesicle endocytosis. *Neurosci. Res.* **2012**, *73* (1), 1−7.
(45) Deguchi, Y.; Donato, F.; Galimberti, I.; Cabuy, E.; Caroni, P. Temporally matched subpopulations of selectively interconnected principal neurons in the hippocampus. *Nat. Neurosci.* **2011**, *14* (4), 495−504.
(46) Jasnow, A. M.; Ehrlich, D. E.; Choi, D. C.; Dabrowska, J.; Bowers, M. E.; McCullough, K. M.; Rainnie, D. G.; Ressler, K. J. Thy1-expressing neurons in the basolateral amygdala may mediate fear inhibition. *J. Neurosci.* **2013**, *33* (25), 10396−404.
(47) Chai, J. H.; Locke, D. P.; Greally, J. M.; Knoll, J. H.; Ohta, T.; Dunai, J.; Yavor, A.; Eichler, E. E.; Nicholls, R. D. Identification of four highly conserved genes between breakpoint hotspots BP1 and BP2 of the Prader-Willi/Angelman syndromes deletion region that have undergone evolutionary transposition mediated by flanking duplicons. *Am. J. Hum. Genet.* **2003**, *73* (4), 898−925.
(48) Wang, C.; Meier, U. T. Architecture and assembly of mammalian H/ACA small nucleolar and telomerase ribonucleoproteins. *EMBO J.* **2004**, *23* (8), 1857−67.
(49) Walne, A. J.; Vulliamy, T.; Marrone, A.; Beswick, R.; Kirwan, M.; Masunari, Y.; Al-Qurashi, F. H.; Aljurf, M.; Dokal, I. Genetic heterogeneity in autosomal recessive dyskeratosis congenita with one subtype due to mutations in the telomerase-associated protein NOP10. *Hum. Mol. Genet.* **2007**, *16* (13), 1619−29.
(50) Kumar, D.; Gokhale, P.; Broustas, C.; Chakravarty, D.; Ahmad, I.; Kasid, U. Expression of SCC-S2, an antiapoptotic molecule, correlates with enhanced proliferation and tumorigenicity of MDA-MB 435 cells. *Oncogene* **2004**, *23* (2), 612−6.
(51) Kumar, D.; Whiteside, T. L.; Kasid, U. Identification of a novel tumor necrosis factor-alpha-inducible gene, SCC-S2, containing the consensus sequence of a death effector domain of fas-associated death domain-like interleukin- 1beta-converting enzyme-inhibitory protein. *J. Biol. Chem.* **2000**, *275* (4), 2973−8.
(52) You, Z.; Ouyang, H.; Lopatin, D.; Polver, P. J.; Wang, C. Y. Nuclear factor-kappa B-inducible death effector domain-containing protein suppresses tumor necrosis factor-mediated apoptosis by inhibiting caspase-8 activity. *J. Biol. Chem.* **2001**, *276* (28), 26398−404.
(53) Vizcaino, J. A.; Cote, R. G.; Csordas, A.; Dianes, J. A.; Fabregat, A.; Foster, J. M.; Griss, J.; Alpi, E.; Birim, M.; Contell, J.; O'Kelly, G.; Schoenegger, A.; Ovelleiro, D.; Perez-Riverol, Y.; Reisinger, F.; Rios, D.; Wang, R.; Hermjakob, H. The PRoteomics IDEntifications (PRIDE) database and associated tools: status in 2013. *Nucleic Acids Res.* **2013**, *41* (Database issue), D1063−9.